EurJIC European Journal of Inorganic Chemistry
ChemPubSoc Europe
MICROREVIEW

DOI:10.1002/ejic.201500598

# Iron Oxide Based Nanoparticles for Magnetic Hyperthermia Strategies in Biological Applications

CLUSTER ISSUE

**Yolanda Piñeiro,*[a] Zulema Vargas,[a] José Rivas,[a] and Manuel Arturo López-Quintela[b]**

**Keywords:** Nanoparticles / Iron / Magnetic properties / Medicinal chemistry / Antitumor agents / Hyperthermia

The use of multifunctional nanoparticles (NPs), usually in the range of 3–100 nm, with their newly discovered properties – such as superparamagnetic (SPM) behaviour, enhancement of activity and selectivity in catalytic processes and localised surface plasmon resonance (LSPR) – offers new technical possibilities for biomedical applications such as magnetic hyperthermia (MH), plasmonic photothermal therapy (PPTT) and enhanced magnetic resonance imaging (MRI). In addition, the small size of NPs presents a unique opportunity to interfere, in a highly localised and specific way, with natural processes involving viruses, bacteria or cells and allows interference in the development of complex diseases like many types of cancer and neuropathies (Alzheimer's, Parkinson's, Kreutzer–Jacobs'). The design of biological applications based on MH is a chemical challenge and core@shell structures are most often used to endow NPs with multifunctional abilities. The success of such MH-based biological applications depends on the magnetic functionality of the core as well as the properties of the surface shell in direct interaction with the biological medium. In this review we will describe the most important methodologies developed to synthesise magnetic core@shell nanostructures and their MH applications.

## 1. Introduction

Magnetic nanoparticles (MNPs) can be manipulated remotely by using an external magnetic field to produce several effects like the magnetic separation of cells, magnetic resonance imaging (MRI), controlled drug delivery, cell and tissue targeting or magnetic hyperthermia (MH).[1–3]

One of the most developed techniques based on MNPs is magnetic hyperthermia in which heat is induced by exposing the target to an alternating magnetic field with the result that tumour cells are killed by ablation ($T$ = 45, 56 °C) or mild heating is induced to trigger biological weakness ($T$ = 40–45 °C). Besides this, the strategy of developing core@shell structures with a predefined set of hierarchical functionalities (loading drugs, permeation, or tagging agents, etc.) allows MH to be used in multipurpose applications that can simultaneously provide MRI images and enhanced drug delivery (EDD) or tissue regeneration triggered by external magnetic excitation (Figure 1).

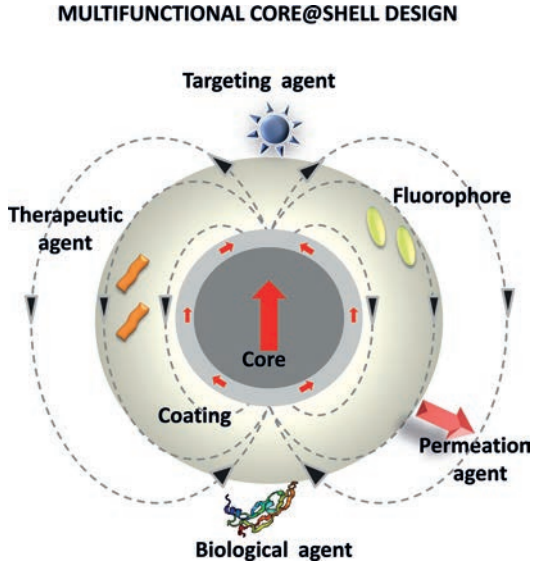


Figure 1. The hierarchical core–shell strategy with magnetic material coated with several agents (polymers, drugs, proteins, etc.) to allow for multipurpose applications.

## 2. Core@Shell Nanoparticles for Magnetic Hyperthermia in Biological Media

The synthesis of hierarchical core@shell MNPs with multiple integrated abilities has to follow designed criteria that incorporate all the relevant facts emerging from three

[a] Applied Physics Department, Faculty of Chemistry, NANOMAG Laboratory, Research Tecnological Institute, University of Santiago de Compostela, 15782 Santiago de Compostela, Spain
E-mail: y.pineiro.redondo@usc.es
zulema.vargas@usc.es
jose.rivas@usc.es
http://www.nanomag.org/grupo_esp.htm
[b] Physical Chemistry Department, Faculty of Chemistry, NANOMAG Laboratory, Research Tecnological Institute, University of Santiago de Compostela, 15782 Santiago de Compostela, Spain
E-mail: malopez.quintela@usc.es
http://www.nanomag.org/grupo_esp.htm

different length scales involved in the whole heat-transfer process:[4]

· the nanoscale, at which the magnetic field is transformed into heat through the interaction with MNPs (5–100 nm) and where proteins (1–100 nm) living in biological media rapidly interact with them;

· the microscale, characterised by the nano–bio interaction of MNPs with cells and their heterogeneous physico-chemical structure (varying composition, viscosity and pH, etc.);

· the macroscale, in which the features of tumours (up to 20 mm), the blood stream and bone structure (pore architecture, intrapore connections, etc.) appear to have heterogeneous physico-chemical conditions.

### 2.1. Nanoscale Elements: Nanoparticles and Proteins

Specifically, MNPs for biomedical applications inside the human body need to combine the following:

· an absence of coercive forces and remanent fields to avoid their magnetic interaction and further agglomeration[1] into large aggregates ($D > 100$ nm) that are readily taken up by macrophages in the blood stream;

· a large magnetic susceptibility that allows for an intense and fast magnetic response minimizing the exposure of the patient to the activating fields.

All of these requirements are fulfilled by superparamagnetic (SPM) NPs. These single-domain MNPs, below a critical size ($D_c$), are characterised by a large total magnetic moment ($M_{SD} \approx 1000\ \mu_B$) undergoing constant thermal fluctuations and giving rise to paramagnetic-like behaviour for temperatures above the so-called blocking temperature, $T_B$.[5]

Different chemical routes (see below) are currently used to provide MNPs with controlled size, shape and crystalline quality to assure optimum magnetic properties. Besides magnetic materials like Co, Ni, Mn or Fe, iron oxide based NPs are the preferred magnetic core choice for in vivo MH applications[6,7] owing to their good magnetic response ($M_{satd.}^{bulk} = 80$–$90$ emu g$^{-1}$), biocompatibility and nontoxicity.

Moreover, besides developing a magnetic core of good quality, several requirements have to be chemically afforded by applying coating strategies to

· prevent the fast oxidation of naked iron-based NPs, which end in a severe loss of magnetic properties or the erosion caused by acids or bases;

*Yolanda Piñeiro began at the Electromagnetic Signature Laboratory (EMSL) in the Joint Research Centre (Ispra, Italy), where her research activities focused on coaxial cable dielectric spectroscopy techniques. She obtained her Masters in Science in Applied Physics in 1997 at the University of Santiago de Compostela (USC). After a training period at UCM (Spain), she obtained her PhD on Lattice Monte Carlo Simulation of complex systems in 2006 at USC (Spain). Thereafter, her major research involves studies on magnetic hyperthermia with superparamagnetic nanoparticle dispersions in different media (liquid, gel and solid) for biomedical applications.*

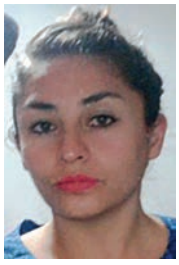

*Zulema Vargas Osorio obtained her degree in chemistry (Faculty of Chemistry, UNAM, 2002–2007, average: 9.16) and her Masters in Materials Science and Engineering (UNAM, 2009–2011). She is a PhD candidate in Materials Science and Engineering (2014) and is currently working on her PhD thesis. With a strong research focus on inorganic synthesis applied to the nanomaterials field, she is working mainly with mesoporous ceramics and magnetic nanoparticles, developing systems for bone tissue regeneration, bone cancer treatment, contrast agents for MRI, control release systems, among other materials.*

*Prof. José Rivas began at Valladolid University (Spain) and the Max Planck Institute (Stuttgart, Germany), where his research activities focused on the preparation and characterization of magnetic materials. He is Full Professor in Physics at the University of Santiago de Compostela (Spain) from 1982, and the major focus of his research is on the synthesis and characterization of nanostructured magnetic materials for biomedical applications, hyperthermia, and biosensors, among others. He is author of several book chapters, 11 patents, and more than 350 scientific articles. He was supervisor of 23 doctoral students and became the First Director General of INL – International Iberian Nanotechnology Laboratory (2008–2014) and was responsible for its implementation.*

*Prof. M. Arturo López-Quintela specializes in the synthesis of nanomaterials by chemical/electrochemical routes. Since 1990 he has been Full Professor of Physical Chemistry at the University of Santiago de Compostela (Spain). He was a postdoctoral candidate at the MPI für Biophysikalische Chemie, Göttingen and at the University of Bielefeld (1980–1984). He was visiting professor at the MPI für Metallforschung, Stuttgart (1990), Centre for Magnetic Recording Research (UCLA, USA) (1992), Yokohama National University (2000, 2003), and Research Centre for Materials Science, Nagoya (2002). He received the Solvay Award in Chemistry (1998). He has been co-Editor of the Journal of Colloid and Interface Science since 2005.*

 

· assure colloidal stability by the electrostatic and steric stabilization of the surface (attractive interactions have to be neutralised to avoid agglomeration of NPs) and avoiding gravitational precipitation;[8]
· endow with biocompatibility [polyacrylic acid (PAA), etc.] and reactive groups for easy functionalization with active biological molecules (target agents, thermoactive polymers, drugs, etc.); physical functionalities like photoluminescence (PL) (fluorophores) or surface plasmonic resonance (SPR) (metal shell) to obtain a multimode MNP with potential application in several areas;
· avoid the plasma proteins (1–100 nm) that favour immune system (IS) recognition, called opsonins [albumin, immunoglobulin (IgG), apolipoproteins, etc.], which adsorb onto the NP surface (opsonization process) after intravenous injection, thereby completely hindering their functionality and allowing their uptake by the phagocytes of the IS (blood monocytes, tissue macrophages, bone marrow progenitors) and clearance (few minutes) to the liver, spleen or bone marrow.[9]

Avoiding protein corona (PC) formation is a crucial step in the rational design of coating procedures since it causes the cancellation of the surface functionalities of the MNPs and prevents the attainment of successful results for in vivo applications. Taking inspiration from the evading ability of erythrocytes (red blood cells), which have a protective shell barrier of hydrophilic oligosaccharide groups,[10] systematic studies varying the NP size, surface charge, coating shell (composition, length, density[11]) and embedding proteins[12] were carried out to analyze the dynamics of PC formation (Figure 2).

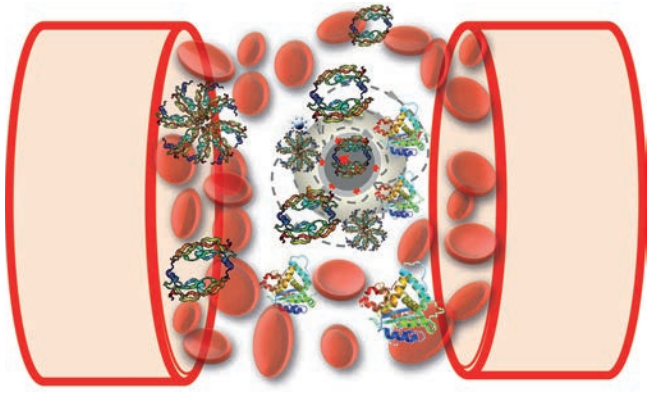

Figure 2. Plasma protein corona (PC) adsorption onto the NPs (opsonization) rapidly forms after intravenous injection and inhibits chemically engineered functionalities of the NP surface.

The main conclusions of such studies were that high surface curvature (small NPs) increases the PC thickness, as well as surface charge and hydrophobicity, whereas a neutral electric surface and hydrophilic coating (large brushes, densely packed[11]) minimise PC formation.[13]

Consequently, hydrophobic NPs need a protective shell of hydrophilic polymer brushes like linear dextrans and their derivatives or poly(ethylene glycol) (PEG); natural molecules such as poly(sialic acid), heparin and heparin polysaccharides or artificial block copolymers like poloxamers [a poly(propylene oxide) (PPO) central hydrophobic block flanked by hydrophilic poly(ethylene oxide) (PEO) blocks] or poloxamines (four PPO/PEO block arms joined by a central ethylenediamine group).[14]

Once the PC formation is minimised, the next step is to implement active targeting procedures for delivering NPs into deep tumour tissues or tagging circulating tumour cells during metastasis. Chemical linking of specific compounds like peptides, proteins (monoclonal antibodies), aptamers, carbohydrates,[15] or also small molecules like folic acid[10] is achieved to tag abnormally expressed proteins or genes (biomarkers) by cancer cells.

### 2.2. Microscale Elements: Cells

Living cells have been defined as a chemically crowded space that behaves like a viscoelastic soft-matter system, in which a permeable membrane contains the cytoplasm gel and the reversible cytoskeleton network.[16] They respond to chemical and physical stimulus by the triggering of specific signalling intermediates,[17] changing their chemical environment, or undergoing biological changes like cell differentiation.[18] Mild oscillating electromagnetic fields (EMF) applied for a sustained time can enhance up to 30-fold the efficiency in reprogramming somatic cells to pluripotent ones[18] or can promote the healing of wounds by triggering anti-inflammatory processes that lead to tissue repair.[19] Magnetic stimulation, thus, widens the range of applications of MH therapies adding the possibility to promote tissue-regeneration strategies.

However, the interaction of MNPs with cells is complex and depending on the physicochemical conditions or the time of exposure, it may also result in the triggering of cytotoxic processes or the internalization of NPs.[13] NP internalization occurs by the intermediation of membrane receptors, proteins or ion channels in two different ways: by endocytosis pathways, which ingest particles below 120 nm inside vesicles that may fuse together forming endosomes in the cytosol; or by phagocytosis of large aggregates, 500 nm, inside large phagolysosomes.[13] By binding ligands to the surface of NPs, one can promote the internalization pathway, that is, transferrin ligands can help endocytosis through clathrin-mediated processes.

And this is the other stage of biological relevance for MH performance. Internalised particles end up in vesicles producing heterogeneously distributed regions with high concentrations of MNP. The influence of concentration on the MH performance is a matter of intense controversy and can produce unexpected effects (see section 2.4). In addition, cell and extracell environments show regions with heterogeneous distributions of largely varying viscosities (illustrated in Table 1) that compromise the mechanic rotation of MNPs and affects MH results.

Table 1. Viscosities of different biological entities.

| Entity | Blood | Cytoplasm | Adipocyte | Extracell matrix | Cancer cells SK-OV-3 |
|---|---|---|---|---|---|
| Ref. | [20] | [21] | [22] | [21] | [21] |
| $\eta$ [mPa s] | 3, 4 | 1, 3 | 36.8 | 200 | 120, 260 |

Finally, the thermal sensitivity of cells, which is the central objective of MH applications, varies within their life cycle. Depending on the thermal stimulation, damage in cell structure or in the chromosomal content can be observed; however, there is a growing amount of experimental evidence showing that 43 °C is the breaking point to enhance cell death.[23] Moreover, owing to rapid metabolic rates, tumour cells are regarded as increasingly vulnerable to hyperthermia effects, showing disruption of nuclear and cytoskeleton assemblies,[23] metabolic signalling processes, protein misfolding and the onset of acidosis or apoptosis caused by the production of heat shock proteins.[24]

### 2.3. Macroscale: Tissues

The third challenge is then to face the chemical and physical diversity of tumour regions. The abnormal replication of cancer cells results in a high rate of vasculature growth with a disordered and imperfect architecture of vessels. Voids in the vasculature favour enhanced extravasations of large particles (between 60 to 400 nm) from the blood stream to the tumour tissue, in which, in addition, an almost absent drainage retains them in the so-called enhanced permeation and retention (EPR) effect.[25]

Moreover, irregular vascularization results in steep oxygen gradients (from 70 to 2.5 torr) with hypoxic areas in deep tumour tissues, combined with an acidic pH generated by accelerated metabolic glycolysis processes.[25]

Consequently, the shell coating of nanocarriers has to be designed to resist oxidative stress and strong acidic environments without suffering from degradation and maintaining the operative conditions of all the loaded agents.

### 2.4. Effects of Viscosity, Coating and Agglomeration Relevant for MH In Vivo Applications

Understanding the fundamentals of MH is crucial to developing realistic biological applications. In the theoretical Rosensweig's approach, the transformation of radiofrequency (RF) ($f$ = 3 kHz, 300 GHz) magnetic energy into heat by MNPs is attributed to Néel (inner fluctuation of the magnetic moment) and Brown (rotation of the whole particle in the embedding medium) relaxation mechanisms for single-domain SPM or hysteresis losses due to magnetic domain and domain wall motion for multidomain ferromagnetic (FM) nanoparticles, respectively.[26]

In this context,[26] the efficiency of a diluted SPM-based ferrofluid for MH design purposes can be computed by the specific absorption rate (SAR), see Equation (1).

$$SAR = \chi_0 H_0^2 \mu_0 \pi \frac{2\pi f^2 \tau}{1+(2\pi f \tau)^2} \quad (1)$$

an intricate relationship between, $\chi_0$, the initial direct current (dc) susceptibility, the alternating magnetic field (amplitude $H_0$ and frequency $f$) and $\tau$, the effective relaxation time that accounts for a combination of Néel ($\tau_N$) and Brown ($\tau_B$) relaxation times, see Equation (2).

$$\tau_B = \frac{3\eta V_H}{k_B T}$$

$$\tau_N = \frac{exp\left(\frac{K_{an}V}{k_B T}\right)}{\sqrt{\frac{K_{an}V}{k_B T}}} \quad (2)$$

Besides some criticisms,[27,28] this approach gives precise predictions of MH performance for ideal ferrofluids in laboratory conditions with homogeneous colloidal properties ($\eta$, the viscosity of the solvent in which the particles are dispersed; $V_H$, the hydrodynamic volume of the particle; $V$, the magnetic volume; and $K_{an}$, the anisotropy constant).

However, in biological media, heterogeneity is the rule, and any MH application will heterogeneously release heat into the therapeutic region. In the following we will highlight the influence in SAR of aspects like the diffusion of heat through the coating; viscosity distribution of the embedding media; and agglomeration of the NPs that produce gradients in the magnetic material concentration. These facts cannot be simply formulated into a theoretical approach and need to be experimentally addressed.

The coating material is a critical parameter for MNPs, not only for their biological fate but also for MH performance. We have recently reported the heating efficiency of magnetite-based water dispersions[29] with the same concentration, $\Phi_{Fe_3O_4}$ = 3 g L$^{-1}$ in which the coating materials (oleic acid, OAc, PAA and $SiO_2$) were shown to strongly affect the SAR values (see Figure 3). The results show a reduction in heating performance for the coated NPs, with remarkable quenching of heat diffusion for the $SiO_2$ coating, which is attributed to the very low thermal conductivity of this material. Gonzalez-Fernandez et al.[30] also reported a similar decrease in MH performance when using silica-coated magnetite NPs.

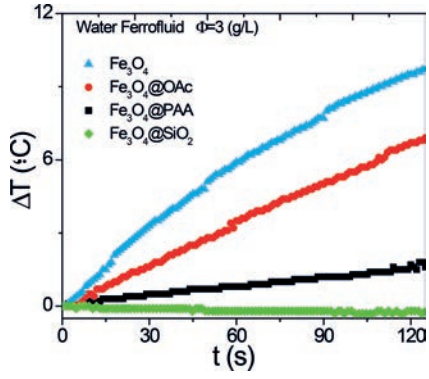


Figure 3. Temperature increase for magnetite coated with different materials with a magnetite concentration of 3 g L$^{-1}$. The graphic is taken from the literature.[29]

 

This result indicates that the interaction of the core and the coating is a crucial design parameter, and to optimise the hyperthermia results the coating thickness of low thermal conductivity materials should be maintained as low as possible since the activity of the MNPs can be completely cancelled.

In a previous work,[31] we attempted a first approximation to identify the behaviour of the SAR with fluid viscosity and MNP concentration, crucial to understand the MH in real biological scenarios. To this end, first we prepared a set of polyacrylic acid coated magnetite ($D_{magnetite}$ = 10 nm) based ferrofluids dispersed in liquids with different viscosities from low (1 mPa s) to high (90 mPa s) over a range of biological areas to test their MH performance under an alternating magnetic field ($B$ = 15 mT and $f$ = 308 kHz).

The influence of viscosity is evident (see Figure 4) and shows an optimum response for medium viscosities and decays for highly viscous environments in which mechanical degrees of freedom are severely restricted. By taking into account that NPs can be immobilised inside tumour cells or immersed in extracellular environments with different viscosities (see Table 1), the heating can be quenched in largely viscous locations, which inhibits the therapeutic effect.

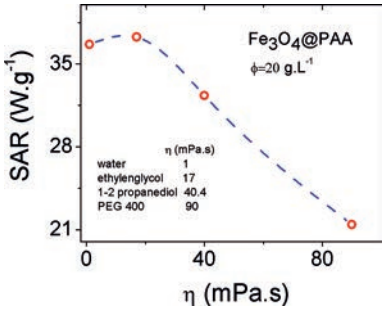


Figure 4. Evolution of the specific absorption rate (SAR) of $Fe_3O_4$@PAA NP dispersions with solvent viscosity ($\eta$) under an external AC magnetic field of $B$ = 15 mT and $f$ = 308 kHz. The solid line is a guide for the eye. The graphic is taken from the literature.[31]

These results lead to the conclusion that since the viscosity of tissues is a parameter outside of the control of the design, magnetic field parameters need to be adjusted to enhance the SAR and cancel out the negative effect of high viscosities in bioapplications.

Another experimental parameter out of the control of the design is the agglomeration of NPs that can happen through cell internalization processes or by shell-coating entanglements. We have recently studied the effect[31] of the concentration on the efficiency of MH (see Figure 5) for bare magnetite and PAA-coated magnetite ($D_{magnetite}$ = 10 nm). The different results can be attributed to the presence or absence of the coating shell that produces agglomerates of nontouching or contacting particles, respectively. It should be highlighted that there is a large controversy in the literature regarding concentration effects on SAR with disparate results, from marginal[33] to sharp variations.[34]

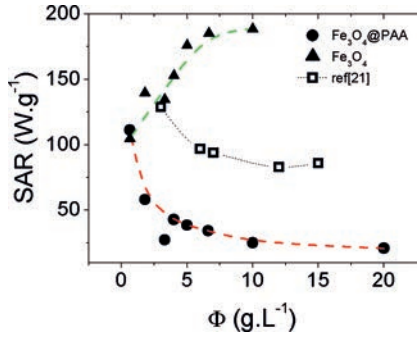


Figure 5. Concentration effect on the SAR of bare magnetite and coated ($Fe_3O_4$@PAA,[31] $Fe_3O_4$@starch[32]) magnetite-based ferrofluids. Coated magnetite showed a decreased MH performance for highly concentrated ferrofluids. The graphic is taken from the literature.[31]

## 3. Synthetic Design of Core@Shell MNPs for Biological Applications

The chemical challenge is to synthesise core@shell MNPs ensuring that (i) in the biological media the magnetic core will not be degraded by the pH conditions, (ii) the therapeutic agents are not lost by simple diffusion before they arrive at the target and (iii) the NPs will be largely retained at the site of therapeutic interest to have enough time to complete all the expected medical actions.

Although there are materials with exceptional magnetic specifications (Co, Ni), their proven toxicity has driven the field to select iron oxide (pure and doped) based NPs as the preferred candidates to develop core@shell structures for biomedical applications owing to their tested biocompatibility and high magnetization. For this reason, the following sections will be exclusively devoted to illustrate the efforts in developing optimum synthetic routes for iron oxide based NPs and their coating procedures.

### 3.1. Synthesis of the Magnetic Core

To find a balance between the need to obtain chemically stable and monodisperse NPs with good structural, morphological and magnetic properties, and the practical requirement of being scalable and environmentally friendly, different modifications of the routinely used wet-chemistry methods have been studied.

In addition to coprecipitation, thermal decomposition, microemulsion and hydrothermal procedures, a new type of biomimetic approach is under development that uses protein cages as biological nanoreactors.

The magnetic quality strongly depends on the degree of order of the crystalline lattice, the oxidation state of iron ions (oxidation of magnetite into maghemite decreases the saturation magnetization value) and the lattice distortion suffered at the surface of the NPs that produces a magnetic dead layer. Therefore, the crystalline quality and adequate oxidation state of lattice metal ions (which can also be optimised by doping with different species) are the relevant aspects regarding synthesis methods.

 

### 3.1.1 Coprecipitation

The coprecipitation of two iron salts in a highly basic aqueous solution with a 1:2 molar ratio of ferric and ferrous ions, at moderate or high temperatures and under an inert atmosphere, is easy, fast and scalable and has become, for this reason, one of the most popular synthetic routes. Although control of the experimental conditions such as the type of $Fe^{2+}/Fe^{3+}$ salt precursors, the $Fe^{2+}/Fe^{3+}$ ion ratio, the pH and temperature results in a good degree of structural (size, morphology) and magnetic properties control, the size distribution obtained with this method is usually wide. This produces ensembles with a large distribution of blocking temperature ($T_B$) values, which is not desired for certain in vivo applications.[35]

This issue has been addressed by the general theory of nucleation and growth, under the so-called burst nucleation approach, which uses supersaturated solutions of the precursors to nucleate in a fast and homogeneous way, giving rise to a monodisperse solution of "nuclei". The subsequent stage of NP growth is controlled to proceed at a slow pace to achieve a final monodisperse ensemble of NPs.[36]

Controlling the reaction atmosphere is also of crucial importance in this method, since magnetite ($Fe_3O_4$) easily oxides into hematite ($Fe_2O_3$), a nonmagnetic (antiferromagnetic) iron oxide phase. Therefore, inert conditions are required to obtain magnetite, or a controlled oxygen atmosphere to obtain, instead of hematite, the other ferrimagnetic oxide, maghemite ($\gamma$-$Fe_2O_3$).

In a recent work, K'olenko et al.[37] reported the synthesis of magnetite NPs of about 13 nm in diameter by coprecipitation under different high-temperature experimental conditions (temperature: 282–363 K; duration: 1–24 h) to optimise the phase purity. The procedure reveals that highly pure magnetite phases are obtained by applying 363 K for one hour with a yield of about 68%, and saturation magnetization ($M_s$) of 72 emu g$^{-1}$, whereas prolonged times result in an over-oxidation leading to NPs with mixed phases magnetite/maghemite with $M_s$ = 50–55 emu g$^{-1}$ or even further reduction in $M_s$ for lower temperatures.

Besides some coprecipitation strategies developed with the addition of surfactants, generally, compounds like dextran, polyvinyl alcohol (PVA) and PAA are added to the reaction in a subsequent step to protect the magnetite NPs from oxidation, control the size, increase biocompatibility and stabilise the colloidal dispersion.

### 3.1.2 Thermal Decomposition

Thermal decomposition of an organic iron precursor phase in the presence of adequate surfactants (fatty acids, oleic acid, oleylamine, etc.) at high temperatures improves the crystalline quality and provides highly monodisperse iron oxide NPs. The temperature of the reaction is adjusted to the solubility of the used solvents, which are usually compounds with high boiling points (octylamine, phenyl ether, phenol ether, hexadecanodiol, octadecene, etc.).

To obtain magnetite/maghemite, the most commonly used iron organic precursors are $[Fe(cup)_3]$ (cup = *N*-nitrosophenylhydroxylamine), $[Fe(acac)_5]$ (acac = acetylacetonate) and $[Fe(CO)_5]$. The routes followed in each case are different. The synthesis using $[Fe(cup)_3]$ or $[Fe(acac)_5]$ as the starting iron precursors consists of their direct decomposition into magnetite/maghemite, whereas $[Fe(CO)_5]$ goes through an intermediate step of metal formation and then oxidation of $Fe^0$ into magnetite by addition of a mild oxidant. Hyeon et al.[38] reported the thermal decomposition of $[Fe(CO)_5]$ in presence of oleic acid at $T$ = 100 °C producing monodisperse iron NPs. In a following step, by adding trimethylamine oxide in a controlled way, maghemite NPs were obtained with tailored sizes between 4 to 16 nm depending on the experimental parameters.

In addition to magnetite/maghemite, this procedure was also applied to synthesise transition-metal oxides (Fe, Mn, Co, Ni, Cr), alloyed compounds ($CoPt_3$, FePt) or metallic (Fe, Ni, Co) NPs.

The most salient advantage of thermal decomposition is that it provides highly monodisperse NPs, although the main disadvantage is that they are generally obtained in nonpolar solvents. Therefore, subsequent phase-transfer strategies are needed to change organic-stabilised NPs into water dispersions.

### 3.1.3 Microemulsion

Microemulsion approaches are based on the formation of a thermodynamically stable isotropic dispersion between two immiscible phases, one hydrophobic and one hydrophilic, with the help of an amphiphilic surfactant that acts as an interface between the two phases and minimises the surface tension; they produce NPs with different morphologies (spherical, cylindrical, lamellar, etc.) depending on the mass ratio of the two phases and the surfactant concentration. The most used microemulsions for the synthesis of NPs are based on water-in-oil (W/O) dispersions in which the water nanodroplets act as nanoreactors and the synthesis takes place in a spatially confined way leading to NPs with a high degree of size and distribution control.

By adjusting three experimental parameters[39] that are interrelated in an intricate way, namely, surfactant film flexibility, reactant concentration and reactant exchange rate, the nanoparticle size, which typically ranges from 1 to 50 nm, can be experimentally controlled. One of the main advantages of this method is that the experimental procedure for microemulsion formation is very simple (just mixing the three components) because microemulsions are well-defined thermodynamic systems.

The NPs synthesis procedure consists of mixing two identical W/O microemulsions, where the reactant solutions of interest (one containing metal ions and the other a reducing agent) are contained inside the microemulsion nanodroplets. The droplets collide, coalesce and finally produce a reactants exchange. At the end of the reaction the nanoparticles have to be extracted by breaking the nanodroplets with acetone or ethanol. Filtering and centrifugation are further needed to obtain clean NPs.

In a previous work,[40] we reported the synthesis of monodisperse maghemite NPs (bare and coated) by a W/O microemulsion using a cyclohexane/Brij97/aqueous phase,

 

which is stable at moderate temperatures. The NPs are formed by coprecipitation of ferrous and ferric salts with two organic bases: cyclohexylamine and oleylamine. Although using cyclohexylamine does not prevent the aggregation of NPs during the synthesis, oleylamine results in a stable colloidal dispersion of oleylamine-coated maghemite NPs. The NPs obtained by using this procedure show a narrow size distribution of 3.5 nm and high saturation magnetization despite being so small (76.3 $A m^2 kg^{-1}$ for uncoated; 35.2 $A m^2 kg^{-1}$ for oleic acid coated; 33.2 $A m^2 kg^{-1}$ for oleylamine coated).

This method, although allowing for morphology, size and distribution control, is operationally very involving and requires several washing and stabilization treatments.

### *3.1.4 Hydrothermal Synthesis*

Hydrothermal synthesis is a simple alternative method to the operationally complicated microemulsion or thermal decomposition processes and provides highly crystalline NPs. The method is based on performing a wet-chemical synthesis in a sealed container at high temperatures (130 to 250 °C) and high vapour pressure (from 0.3 to 4 MPa) for long periods of time (up to 72 h) with the aim of growing dislocation-free crystalline lattices.

Kolen'ko et al.[37] reported a hydrothermal method to produce coated magnetite with sizes of around 20 nm with high yield (around 86%) by mixing $FeCl_2{\cdot}4H_2O$ and $FeCl_3{\cdot}6H_2O$ and keeping it at 473 K for 24 h in a Teflon® vessel with either an oleate or a PAA solution to produce oleate-coated $Fe_3O_4$ and PAA-coated $Fe_3O_4$, respectively. The obtained NPs show a high degree of crystallinity and superior magnetic quality, $M_s$, as high as 84 emu $g^{-1}$.

In another approach, Daoud et al.[41] presented the synthesis of magnetite NPs with an unusually large size for hydrothermal treatments, nearly 39 nm in size, with rounded cubic shape. The procedure comprises the coprecipitation of ferrous $Fe^{2+}$ and ferric $Fe^{3+}$ ions by N-$(CH_3)_4OH$ solution at 70 °C, followed by a thermal treatment at 250 °C for 24 h. The saturation magnetization measured before and after the thermal treatment was found to be 59.8 and 82.5 emu $g^{-1}$, respectively, and clearly shows the improvement of the crystalline and magnetic qualities by annealing at high temperatures.

### *3.1.5 Protein Cages*

The use of protein cages is a new synthetic approach based on biomineralization strategies with different types of proteins, which allows the synthesis of so-called biogenic magnetite. Small ferrihydrite NPs can be mineralised inside ferritin (Fn) cages with large size and shape control under mild biological conditions. Ferritin is an ubiquitous protein present in almost all living organisms and, besides some differences in the amino acid sequences, they all share a common spherical shape composed of 24-subunit proteins self-assembled into a cagelike architecture that sequesters toxic $Fe^{2+}$ in its interior and transforms it by oxidation into an innocuous iron oxide mineral. Although the reaction can be simply written as shown below, the whole process is biologically and chemically complex.[42]

$$4Fe^{2+} + O_2 + 6H_2O \xrightarrow{\text{yields}} FeOOH_{core} + 8H^+$$

The pioneering work of Mann et al.,[43] which demonstrated that magnetite NPs could be artificially synthesised inside empty ferritin (apoferritin) at high temperature and pH, opened the way to a new biomimetic synthesis strategy. This method is based on the use of hollow biological cavities as templates to perform a constrained reaction to produce monodisperse NPs with controlled size and shape under experimental conditions that assure high crystallinity.

Ferritins from different animal sources, as well as different proteins of the ferritin-like (Fn) superfamily (i.e., DNA-binding protein from nutrient-starved cells) or virus capsids, which also show cagelike structures with available sizes in the range from 18 to 500 nm, have been used since they resist higher reaction temperatures and control the size of the produced NPs over a wide range.

Fantechi et al.[44] reported the synthesis of Co-doped magnetite within a genetically modified human Fn cage carrying an α-melanocyte-stimulating hormone peptide. Monodisperse NPs with an average diameter of 7 nm and a large maximum saturation magnetization of 96 $A m^2 kg^{-2}$ at room temperature can be obtained, which are very interesting for MH and MRI enhancement.

Parker et al.[45] reported the use of *Pyrococcus furiosus* (Pf)-Fn to synthesise maghemite NPs at different temperatures and iron salt concentrations to obtain highly monodisperse MNPs with sizes between 4.5 and 6.9 nm and small coercive fields – between 60 and 250 Oe, respectively – depending on the experimental conditions. In addition, NPs synthesised in Pf-Fn display rapid saturation well below 1 T, which is much lower than that for NPs synthesised in human Fn cages (above 6 T).

## 3.2. Synthesis of the Outer Shell

Surface features are of paramount importance since they are in direct contact with physiological fluids and cells. Its modification can be afforded by complex or one-step strategies comprising surface passivation by controlled mild oxidation of the outer surface; surfactant and polymer coating; or inorganic coating (silica, carbon, noble metals).[46]

### *3.2.1. Oxidation*

Mild oxidation consists of the controlled oxidation of a thin external surface layer on the NPs to protect the whole particle from massive and uncontrolled oxidation. Lee et al.[47] reported the synthesis of Fe MNPs by thermal decomposition of $[Fe(CO)_5]$ followed by controlled oxidation in air to grow a narrow ferrite shell, which results in monodisperse core–shell Fe-ferrite NPs with core diameters of 11 nm, shell thicknesses of 2.5 nm, high saturation magnetization ($M_s$ = 139 emu $g^{-1}$) and good crystalline quality (see Figure 6).

 

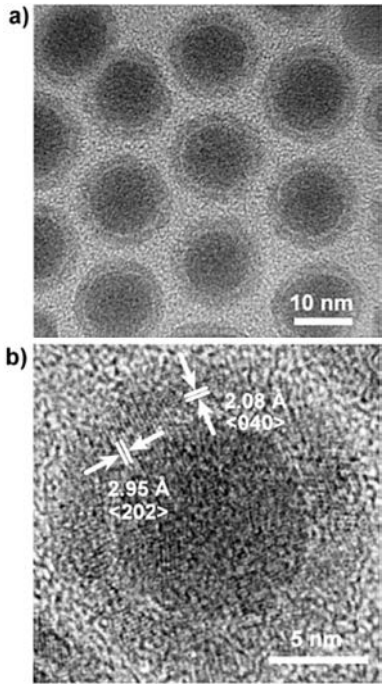


Figure 6. Mild oxidation of Fe NPs into Fe@$Fe_3O_4$ NPs for which high-resolution images evidence (a) the core diameter (11 nm) and the shell thickness (2.5 nm) of highly monodisperse NPs and (b) the multiple domains of single crystals of the shell produced by the mismatch between the Fe core and iron oxide shell. Figures are taken from Lee et al.[47]

### 3.2.2. Surfactants

Small organic molecules or surfactants can be categorised into three groups: oil soluble (e.g., alkyl phenol, oleic acid, etc.) having a weak attraction for the solvent; hydrophilic (e.g., ammonium salt, polyol, lycine, etc.) having a strong attraction for the solvent environment; and amphiphilic (e.g., sulfuric lycine) that are endowed with oil and water solubility.

The presence of hydroxyl groups, Fe–OH, greatly facilitates the anchoring of different compounds: alkoxylanes, carboxylic acids, phosphonic acids, dopamine, and so forth.

In situ coating is a popular route, since it requires no further procedures after the whole NP synthesis. One method consists of directly adding small biocompatible compounds (amino acid, citric acid, vitamins, cyclodextrin) to the main core synthesis. However, the colloidal stability is not good and decomposition of the small organic compounds in basic or acidic media can be observed.[48] In this regard, coating with several commercially available silane groups is becoming increasingly popular since they show good water stability, no cytoxicity and can be covalently attached through the reaction of surface Fe–OH groups with Si–$OCH_3$, by one-pot procedures[49] or by direct addition onto the NP core.[50] 3-Aminopropyltriethyloxysilane (APTES) and mercaptopropyltriethoxysilane (MPTES) agents are mostly used[49] to provide amino and sulfhydril functional groups, respectively, for bonding with different bioactive compounds (i.e., small carbohydrates[15] or drugs like ciprofloxacin or ofloxacin[50]) on the NP surface together with a negligible loss of magnetic properties.

Carboxylic acid groups can interact with the NP surface by coordination processes and this is commonly used in organic solvent synthesis, although this bond is thermally weak. Phosphonic acid forms an Fe–O–P bond that ends up with a higher grafting density than carboxylic bonds, and, together with dopamine groups, which bond through orbital overlap, provides improved pH and temperature stability to the iron oxide core than other groups.[15] Shahoo et al. reported an efficient coating of 6–8 nm magnetite NPs by oleic acid, lauric acid, phosphonic acids (dodecyl-, hexadecyl-) and dihexadecyl phosphate, thereby showing that the bonding strength of alkyl phosphonates and phosphates is stronger than that of carboxylate, and proposed it as a biocompatible alternative to fatty acids for coatings in organic solutions.[51]

Oleic acid [$CH_3(CH_2)_7CH{=}CH(CH_2)_7CO_2H$] is not only one of the most used oil-soluble coatings for magnetite, but can also be referred to as an example of steric stabilization. This fact has been attributed to its *cis* double bond, which forms a kink in the middle of the carbon chain structure. In comparison, stearic acid [$CH_3(CH_2)_{16}CO_2H$], which has no kinks, has no ability to stabilise iron oxide NPs.[52] Besides this fact, oleic acid shows an interesting ability to enhance the magnetic properties of very small magnetite NPs. Guardia et al.[53] performed a thermal synthesis of OAc-coated $Fe_3O_4$ NPs with different sizes (6, 10 and 17 nm) that present saturation magnetization values $M_s$ ($T$ = 5 K) of 79, 81, 84 emu $g^{-1}$, respectively, that are very close to the bulk value of $M_s$ = 92 emu $g^{-1}$. In contrast, similar bare $Fe_3O_4$ NPs of 4 nm display only $M_s$ = 50 emu $g^{-1}$. The observed enhancement supports the idea that OAc molecules are covalently bonded to NPs, thereby reducing the surface spin disorder, and thus, the dead magnetic surface layer, which makes this material of great interest for coating and enhancing the magnetic performance of ultra-small iron oxide NPs.

However, although many of the synthetic procedures for obtaining monodisperse magnetite NPs take place in organic solvents,[35] biomedical applications require water-soluble preparations and different strategies have been developed to perform the NP phase transfer, such as surfactant addition, surfactant exchange of initial oil-soluble surfactants or in situ procedures.

The addition of amphiphilic molecules to the oil-soluble phase is a primary strategy in which the hydrophobic segments form a robust double layer with the hydrophobic tail of the initial coating, and hydrophilic segments remain exposed to the solvent.[54]

Surfactant exchange replaces the initial surfactant with a new bifunctional surfactant, which has one group capable of binding to the NP surface by a strong chemical bond, and the other terminal group, which is polar, remains exposed to the water. Sun et al.[55] reported the synthesis of magnetite NPs by means of a high-temperature phase reaction of $Fe^{III}$–acetylacetonate, [$Fe(acac)_3$], with 1,2-hexadecanediol in the presence of oleic acid and oleylamine. Tun-

 

able sizes were obtained, between 3 and 20 nm, of oil-soluble $Fe_3O_4$ NPs, which after mixing with tetramethylammonium 11-aminoundecanoate were transformed into stable water-soluble dispersions.

Fan et al.[56] reported the synthesis of $F_3O_4$@bipy NPs with a diameter of 13 nm by means of site exchange of oleic acid coated $Fe_3O_4$ in $CHCl_3$ with *N*-methyl-*N*′-(5-carboxypentyl)-4,4′-bipyridium iodide bromide salt. The presence of bipyridium ligands increases the water solubility of the ferrofluid up to 300 mg mL$^{-1}$, and more interestingly, it enhances the stability of magnetite in a wide range of pH conditions (see Figure 7) from very acidic (pH 1) to very basic (pH 11). This point is extremely useful to prevent magnetite from dissolution in acidic media, for example, tumour locations, for which therapeutic procedures require the long-term stability of $Fe_3O_4$ NPs.

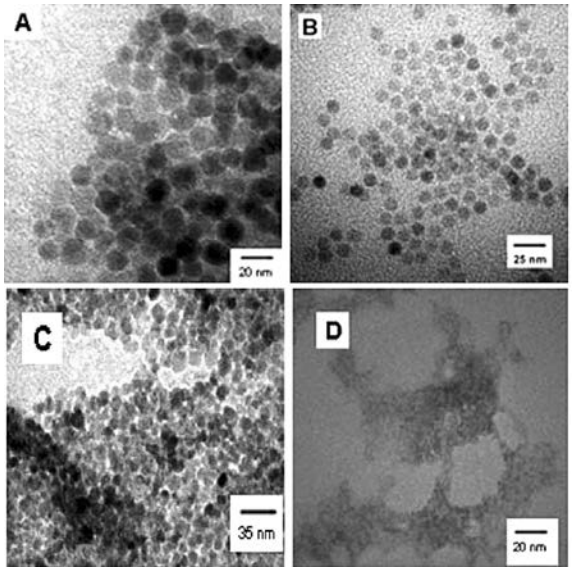


Figure 7. TEM images of bipyridium–$Fe_3O_4$ NPs from the buffer solutions at pH (A) 3, (B) 7, (C) 9, and (D) 11. The graphics are taken from the literature.[56]

### *3.2.3. Polymers*

Polymers provide high colloidal stability due to the large number of repulsive groups balancing the attractive magnetic and van der Waals interactions that cause the agglomeration of NPs. In addition, they are preferred for medical applications since they increase the prevention of opsonization processes and offer a surface with a large number of functionalization possibilities for combining multiple abilities (tracking circulating cells, targeting specific tumour regions, delivery and stimulated release of therapeutic agents or facilitate cell internalization).

Natural polymers like dextran, chitosan, starch, gelatine and their derivatives were the first used because they are inexpensive, biocompatible and present a low immunogenic response. However, to expand the application range, strategies based on synthetic functional polymers were also developed, such as linear or brush structures such as PEG, PVA, polylactic acid (PLA), polyvinylpyrrolidone (PVP), PAA, and so forth. Two alternative approaches were used to graft from and graft onto the NPs.

"Grafting from" strategies are based on fixing monomer ligands to the NP surface, which, after polymerization, gives rise to a very dense shell coating. However, with this method the final polymeric structure cannot be completely controlled and the magnetic core is exposed to organic solvents with the risk of degradation.[15] To avoid these problems, protocols are under development. For example, Lattuada et al.[57] reported the use of carboxylic groups to perform a grafting-from strategy by atom-transfer radical polymerization (ATRP) or ring-opening polymerization (ROP) using different hydrophilic and hydrophobic polymers.

"Grafting onto" consists of grafting a preformed polymer onto the NP surface by using in situ procedures. This strategy allows a strict control of the polymer architecture and functionality, although the density of grafting is poor. In a recent work,[31] we reported in situ PAA grafting onto $Fe_3O_4$ NPs with good MH performance, high colloidal stability and interesting functionalization abilities for biological molecules.

However, all of the preceding methods are complex and there is a need to develop simple procedures to produce coated NPs in a single step.

One-pot syntheses have been explored by different routes to obtain size-controlled magnetite NPs by also using the coating polymer as a stabilizing agent. Poly(styrene-*alt*-maleic acid) (PSMA),[58] an amphiphilic block copolymer, is one of the most used as a coating agent and stabiliser in different one-pot green syntheses by mixing it with different metal salts to produce polymer-coated NPs (Au, Ag, Cu, $Fe_3O_4$ and $TiO_2$)@PSMA with different morphologies (single core to multicore).

Lu et al. prepared[59] PVP-coated $Fe_3O_4$ nanocrystals by a "one-pot" synthesis through the pyrolysis of ferric triacetylacetonate {[Fe(acac)$_3$]} in *N*-vinyl-2-pyrrolidone (NVP). The resultant PVP-coated $Fe_3O_4$ NPs presented super-dispersability in ten different types of organic solvent and different aqueous solutions with pH ranging between 2.0 and 11.0, and a stable hydrodynamic size of around 20 nm. This enhanced colloidal stability under a wide range of solvents and pH conditions makes PVP coating desirable for its resistance to the physicochemical conditions of cancer tissues.

Lutz et al.[60] reported the use of well-defined poly[oligo(ethylene glycol)methacrylate-*co*-methacrylic acid] [P(OEGMA-*co*-MAA)] copolymers as coating agents and stabilisers by its simple addition into a coprecipitation of $Fe^{II}$ and $Fe^{III}$ chlorides mixed with an ammonium hydroxide solution under an argon atmosphere. Polymer-coated $Fe_3O_4$ NPs with controlled sizes (from 10 to 25 nm) were obtained by varying the amount of P(OEGMA-*co*-MAA).

The need to minimise protein adsorption on the MNP surface led to a new line of research based on PEG coating strategies: so-called PEGylation. Gref et al.[11] presented a complete study of protein adsorption for varying brush types and amounts of PEG coating on polymer NPs (with a PLA, PCL or PLG core). The PEG molecular weight [MW (chain length)] was varied between 2000 and 20000 g mol$^{-1}$

 

and the PEG weight content (wt.-%) was varied between 0.5 and 50. The influence of chain length is clear: opsonization decreases from 1600 counts per million (cpm) for noncoated NPs to an almost constant value, 400 cpm for PEG $M_W$ = 5000 g mol$^{-1}$ and beyond, which shows that PEGylation can hinder but not completely prevent proteins adsorption. Density also plays an important role: Above 5% PEG coating, opsonization remains constant below 400 cpm, therefore showing an interdistance threshold of 1.0 nm between terminal PEG brushes to avoid adsorption of small proteins (see Figure 8).

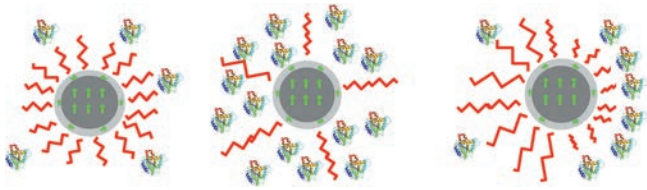

Figure 8. High densities of grafting and large polymer brushes strongly diminishes the protein corona formation.

However, the grafting decoration with PEG brushes induces a competition between the ability to minimise PC formation and the tagging ability, as sketched in Figure 9 (a, b). In a recent work, Dai et al. presented a study of NPs grafted with different decorations of PEG brushes (see Figure 9) exposed to human serum. The combination of a backfilling of short PEG together with large PEG tethers conjugated to target ligands (herceptin conjugated to alexa fluor 647) as shown in Figure 9 (c) allowed for optimum tagging abilities in combination with a strong suppression of PC formation.

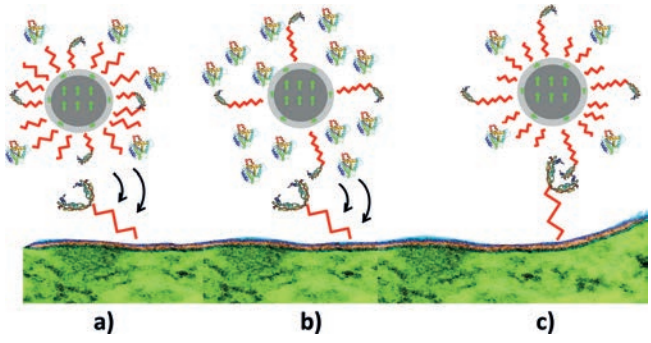


Figure 9. The surface decoration with PEG has an important impact on tagging abilities and opsonization hindrance: (a) short tethers or (b) large tethers without backfilling are unable to minimise opsonization, whereas (c) backfilling and long tethers avoids opsonization and maintains tagging abilities.

Specially interesting are those stimuli-responsive polymers that under pH, temperature or light irradiation variations undergo conformational changes that can be used to provide controlled delivery and release of loaded drugs.[61] Specifically, from the point of view of MH applications, thermoresponsive polymer hydrogels like Pluronic, poly(*N*-isopropylacrylamide) (PNIPAM) and their derivatives (e.g., PNIPAM with chitosan,[62] etc.) doped with magnetite NPs, which act as heat sources, are the most studied hybrids.

At a certain temperature (lower critical solution temperature, LCST) these polymers undergo a coil-to-globule transition and can expel any loaded molecule due to the shrinking of the network. Interestingly, Dionigi et al.[63] reported the synthesis of PNIPAM sponges by surfactant-free radical polymerization under controlled pH, loaded with different water dispersions of magnetite NPs showing a tunable LCST controlled by the MNP concentration loading.

### 3.2.4. Inorganic Materials

Inorganic shells (noble metals, silica and carbon) are widely used materials for biomedical applications. Besides offering colloidal stability to aqueous dispersions or an easily functionalizable surface, they allow control of the magnetic interparticle interactions by tailoring the shell thickness.

From all metals, gold is mostly chosen for its low reactivity, high biocompatibility, the ability to bind to thiol groups (–SH) (favouring the binding of biological molecules) and its surface plasmon resonance (SPR), which provides an additional imaging possibility for hybrid gold–magnetic NPs. The main difficulty in coating MNPs with gold is the mismatch between the crystalline lattices of both phases (magnetic core and gold), with the exception of the perfect matching of Fe/Au lattices (see Figure 10).

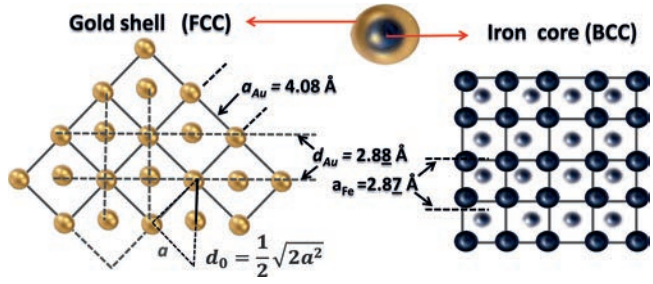


Figure 10. Minimal crystal lattice mismatch at the gold–iron interface. Gold interplanar distance, $d$ = 2.88 Å, is almost equal to the lattice constant of iron, 2.87 Å.

In a recent work, we reported[64] the synthesis of small Fe@Au NPs (6 nm) by a microemulsion method that showed a high degree of crystalline quality (Figure 11, b) and complete iron-core coating by the gold shell as further confirmed by the SPR of a colloidal dispersion with water and MUA ($\lambda$ = 534 nm), which is almost similar to spherical Au NPs ($\lambda$ = 520 nm; Figure 11, a). By tailoring the thickness of the gold shell, one can change the location and wideness of the resonance peak, which is interesting for applications in which magnetic and optic responses may be required.

However, for the coating of magnetite by gold crystal mismatch is a problem and gives rise to different effects. Smolenski et al.[65] prepared small $Fe_3O_4$@OAc particles (4.8 nm) by thermal decomposition of [Fe(acac)$_3$] in the presence of OAc and oleylamine and achieved $Fe_3O_4$@Au

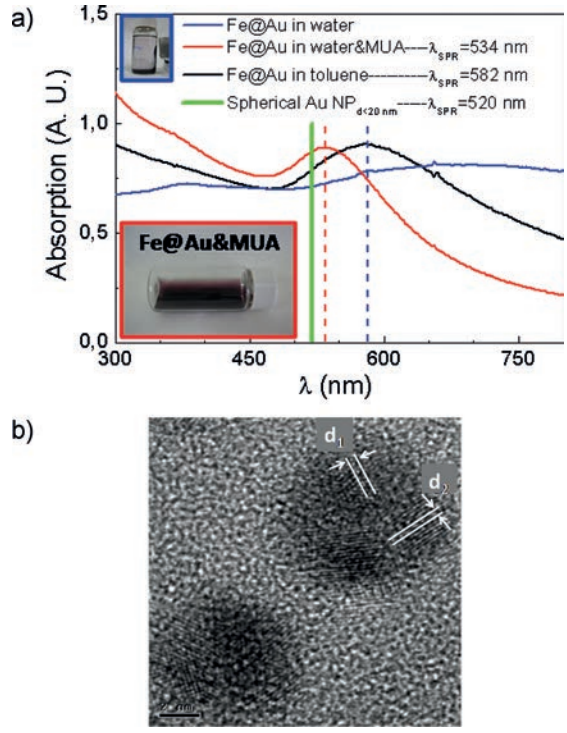


Figure 11. (a) UV/Vis absorption of Fe@Au NPs dispersed in three different solvents: water; a mixture of water and MUA (thiol) and toluene. (b) High-resolution TEM image, which reveals high crystallinity with different fringes revealing two interplanar distances, $d_1$ = 2.4 Å and $d_2$ = 2.0 Å corresponding to gold planes (111) and (200) and iron (110), respectively. Images taken from the literature,[64] copyright Springer 2013.

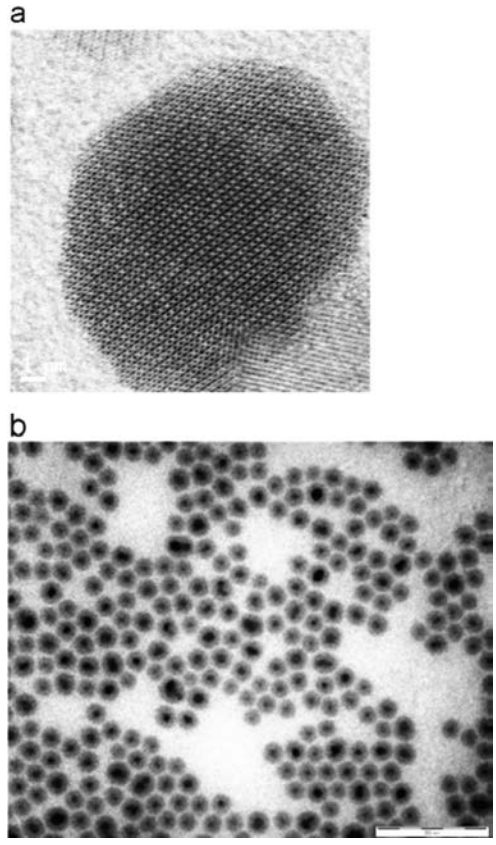


Figure 12. (a) HRTEM image of PAA-coated magnetite, 10 nm, and (b) TEM image of silica-coated magnetite NPs. The graphic was taken from the literature.[29]

(80 nm) by replacing OAc with 3-aminopropylphosphonic acid and sonicating in $HAuCl_4$. The hybrid gold-coated magnetite was reported to show a lower saturation ($M_{sat}$ = 81 A m$^2$ kg$^{-1}$) than that of $Fe_3O_4$@OAc ($M_{sat}$ = 92 A m$^2$ kg$^{-1}$) due to Au-ion diffusion into the $Fe_3O_4$ lattice causing magnetic disorder. In contrast León-Félix et al.[66] reported the synthesis of $Fe_3O_4$@Au (8 nm) by coprecipitation of iron salts, and further thermal treatment in the presence of $HAuCl_4$ to develop the Au coating shell. In this case a slight increase in magnetic saturation was observed, which is attributed to the recrystallization of magnetically disordered regions on the surface of the magnetite NPs.

Silica ($SiO_2$) coating is commonly performed by a sol–gel process with the help of two organosilanes, tetraethyl orthosilicate (TEOS) or 3-aminopropyltriethoxysilane (APTES). The process consists mainly of the basic hydrolysis of silanes in aqueous solutions. The reaction between the oxide surface and the silica takes place by the OH groups[35] and the procedure allows control of the shell thickness of silica by adjusting the amount of added TEOS. In addition, two different routes can be followed: Stöber processes, which generally result in a multicore coated NPs, and microemulsion processes, which provide mainly core–shell NPs.[67] In a recent work,[29] we reported the synthesis of highly monodisperse core–shell $Fe_3O_4$@$SiO_4$ by a modified Stöber method, which provided NPs with a high degree of crystal quality as shown in Figure 12.

## 4. MH-Based Applications with Core–Shell NPs

Besides some criticisms[68] about MH viability for real applications, which are an interdisciplinary task of enormous complexity, progress in this field has evolved continuously and significant steps have been made to address important questions, such as the biological fate of MNPs inside biological media, the optimum conditions to attain the desired SAR, and so forth. The field is entering into a stage of maturity, where the different aspects of MH mechanisms are better known, the nano–bio interaction is more deeply understood and new biochemical routes have been developed to synthesise NPs with multimode abilities that include imaging possibilities or bioresorbable magnetic materials for tissue-engineering-combined applications.

### 4.1. MH-Based Applications

Killing tumour cells by heat application in a very localised way with a minimum risk for healthy nearby cells is the first application of MH. Besides the large list of different works one can find in the literature, MagForce, a fully operative clinical therapy based on aminosilane-coated $Fe_3O_4$ NPs together with a magnetic actuator for treating brain cancer, is considered a milestone in the field.

The MagForce AG (Berlin, Germany) Nanoactivator[69] produces 100 kHz magnetic fields that can, in principle,

 

treat tumours of about 5 cm after injecting 3 mL of a simple core–shell $Fe_3O_4$@amilosane ferrofluid into the patient and has been used in a phase II clinical trial to test MH in combination with stereotactic radiotherapy. It obtained European approval in 2010 for brain-tumour treatment after demonstrating its capability to increase life expectancy from 6 to 13 months in patients with glioblastoma multiform brain cancer relative to those subjected only to chemoradiotherapy. Phase I clinical studies are also being carried out on prostate cancer to explore the benefits of MH in this heterogeneous and multifocal modality of cancer.[70]

However, to tag different types of cancer cells more sophisticated MNPs are required. Fantechi et al.[44] reported the synthesis of Co-doped magnetite within a PEGylated genetically modified human Fn cage carrying a α-melanocyte-stimulating hormone peptide that has excellent targeting properties towards melanoma cells. The resulting MNPs showed an extremely small size constrained by the cage, about 7 nm, with high magnetic efficiency due to Co doping. In vitro tests performed on a B16 melanoma cell line cultured with these Co-doped magnetite NPs showed an advanced stage of apoptosis after performing a MH treatment ($f$ = 128 kHz; $B$ = 12.4 kA m$^{-1}$). This system is a promising candidate for a protein-based theragnostic platform.

Other diseases different from cancer, such as neurodegenerative disorders, have also been explored by combining MNP strategies to achieve early detection, which is one of the major problems in this disease, although classifying criteria have not been clearly established. Fibril-forming proteins, insulin and amyloid-β 40 ($A\beta_{40}$) are candidates for such early detection and selective marking by MNPs. Skaat et al.[71] reported the use of fluorescent maghemite NPs (15 nm), synthesised by nucleation, for detecting the onset of fibril formation by exploiting their ability to tag fibril-forming proteins, that is, insulin and $A\beta_{40}$. Fluorescent maghemite NPs embedded in sets of insulin and $A\beta_{40}$ aqueous phases, selectively linked to insulin and $A\beta_{40}$, respectively, interfere with the fibrillation process. The fibrils were marked by fluorescent dyes (rhodamine and fluorescein) allowing for imaging, and could be removed by magnetic interaction. Furthermore, coating maghemite NPs with a fluorinated polymer [poly(2,2,3,3,4,4,4-heptafluorobutyl acrylate)] revealed a delay in the appearance of the fibrillation process up to 20 hours. Another approach is to fight tau dysfunctions, which are suspected to be behind many disorders like Alzheimer′s disease, Pick's disease or Parkinsonism. In a recent work, Glat et al.[72] demonstrated the beneficial effect of a fibrin peptide conjugated to γ-$Fe_2O_3$ (maghemite) in reducing the activation of microglial cells in rTg4510 mutant mice, which resulted in a reduced number of neurons with the undesired tangles compared to animals not treated with the therapeutic nanoparticles.

### 4.2. Combined MH and Controlled Drug Delivery

Thermoresponsive polymers, like Pluronic or PNIPAM are a natural combination with magnetic nanoparticles to provide drug delivery. Thermoresponsive polymers can be charged with therapeutical agents capable of retaining the drug at body temperature and then release it under hyperthermia conditions by controlled external magnetic stimulation.

Poly-*N*-isopropylacrylamide is a LCST-biocompatible and thermoreversible polymer that can produce hydrogels that undergo a coil to globule collapse at temperatures above 32 °C. Dionigi et al.[63] have been able to regulate the thermal response of PNIPAM by controlling the adsorption of $Fe_3O_4$ NPs, which show that LCST can be tuned in a range from 32 to 50 °C by controlling the amount of MNP doping between 40 and 70%. Interestingly, at 49% doping, shrinking at body temperature ($T$ = 38 °C) is achieved. PNIPAM, synthesised by surfactant-free radical polymerization, was loaded with a water dispersion of MNPs under controlled pH, and was further tested in MH experiments ($f$ = 293 kHz, $B$ = 30 mT). It was found that in less than four minutes, maximum temperature increases of up to 40 °C can be obtained, which are in the range of the expected expulsion threshold.

Regmi et al.[73] loaded PNIPAM/magnetite composites with mitoxantrone, an anti-cancer drug, and succeeded in producing enhanced drug release by applying MH with a magnetic field of 130 Oe and 380 kHz. With different compositions of PNIPAM/magnetite loaded with mitoxantrone, they achieved a mild hyperthermia from 298 K up to 323 K in only four minutes, and a controlled release of the drug up to the 4% of the total.

In a very recent work, Yadavalli et al.[62] presented a polymer complex made of PNIAM–chitosan, doped with $NiFe_{1.8}Gd_{0.2}O_4$ ($M_{sat}$ = 40 emu g$^{-1}$) and loaded with curcumin (anticancer drug). The active drug release under MH stimulation ($f$ = 250 kHz, $B$ = 35 mT) shows a very promising performance, and produces a burst release of 70% of the loaded drug, at 45 °C, in less than one second and in addition, it has the potential to be used as an MRI contrast agent.

### 4.3. MH Combined with Tissue Engineering

Cancer metastasis affects bones in 70% of patients with a prostate or breast primary cancer diagnosis, and about 30% of those with a thyroid, kidney or lung primary diagnosis. Therefore, many efforts are devoted to address new strategies in MH that could overcome the difficulties related to this specific type of cancer: the deep location of bone in the body; its low thermal conductivity; the thickness of cortical bone and the high vascularization of the medulla.[74]

Related to bone cancer, fractures are a secondary effect that lower quality of life and are being addressed by implantation of porous scaffold materials [polycaprolactone (PCL), hydroxyapatite (HA), collagen, etc.] with good mechanical performances and biometric pore distribution to allow osteogenesis and vascularization. Promoting biological functionality of the osteogenesis and vascularization of scaffolds is of crucial importance, for which different strategies like magneto-mechanical stimulation, heat application or release of bioactive molecules [vascular endothelial growth factor (VEGF)][75] have been proposed.

 

The beneficial effect of mild hyperthermia has been reported by Chen et al.[76] with in vitro studies of conventional 2D and PuraMatrix 3D cultures of human mesenchymal stem cells (hMSC), relevant for bone tissue engineering. Exposure to heating cycles ($T$ = 41 °C, over 1 h for several days) showed an early osteogenic differentiation of osteoblasts under these conditions.

The combination of magnetic stimulation with heating abilities is being addressed by a new generation of magnetic scaffolds (MAGs) showing a set of appealing abilities: to induce mild hyperthermia for enhancement of vascularization processes or selectively promote cell differentiation;[73] to kill residual bone tumours by ablation; to provide magnetic guidance of injected magnetic nanocarriers or allow for new magnetic fixation on the body.[77]

We have recently reported in a series of related works[77–80] the development of a set of new MGs comprising hybrid hydroxyapatite (HA)/polycaprolactone (PCL)/MNP scaffold materials or bioresorbable magnetic scaffolds[78] [iron-doped HA (FeHA)], which has been bioplotted into two-dimensional and three-dimensional shapes with controlled geometries and pore distribution. Hybrid 2D and 3D scaffolds PCL/FeHA show that a 10% doping with FeHA reinforces the mechanical response of the PCL structure confirmed by small punch tests (displacements at maximal loads from 15 to 22.51 N, respectively).[79] In addition, the magnetic performance is good and assures temperature increases of about 15 °C in less than five minutes under MH tests.[79] Also, in vitro tests with hMSC show adhesion and spreading in a few days. Furthermore, in vivo tests of these 3D MAGs have shown to enhance tissue regeneration in a critical-size lesion of a rabbit condyle[81] and to allow for magnetic fixation through the implantation of permanent NdFeB magnets.[82]

### 4.4. Combined MH and Enhanced MRI

There are a set of frequently employed noninvasive imaging techniques for clinical use that are key tools for early detection and screening of serious diseases, like MRI, X-ray computed tomography (CT), positron emission tomography (PET), or ultrasound (US), which can benefit from technological improvements by using multimodal magnetic nanoparticles for imaging enhancement. Different designs can be afforded either by combining several agents into a single carrier, or by engineering a material that can be active in more than one modality.[83]

To avoid the use of highly toxic Gd for MRI, magnetite and doped variants are emerging as the materials of choice in magnetic applications due to their good response and biocompatibility. Many efforts have been devoted to enhancing their magnetic response to minimise the dosage of contrast agents. The most followed strategy is the modification of intrinsic properties of magnetite by doping with Zn, Ti, Co, Ni, and Mn, by controlling the generation of non-stoichiometric or metastable states in which metal ions are disordered in the $T_d$ and $O_h$ sites of the magnetite lattice, to avoid reduction of the magnetic response.

Jang et al.[84] presented a systematic study based on zinc-doped iron oxide nanocrystals (ZnNCs), synthesised by a thermal decomposition approach, showing a fourfold increase in hyperthermia and an eightfold increase in MRI contrast compared to pure iron oxide NPs. Specifically, contrast is reported to depend on the dopant metal and doping concentration, $x$, in $(Zn_xMn_{1-x})Fe_2O_4$ and $(Zn_xFe_{1-x})Fe_2O_4$, and the relaxivity coefficient $r_2$ [$mM^{-1}s^{-1}$] largely overpasses the values reported for commercial contrast agents (Feridex: $r_2$= 110 $mM^{-1}s^{-1}$; CLIO: $r_2$= 62 $M^{-1}s^{-1}$), showing at $x$ = 0.4 a maximum response (see Table 2). In addition, $(Zn_{0.4}Mn_{0.6})Fe_2O_4$ NPs were embedded into HeLa cultured cells, and MH experiments were performed that demonstrate that up to 84.4% of cells were killed after the treatment.

Table 2. Saturation magnetization ($M_s$ in emu $g^{-1}$) and relaxivity [$mM^{-1}s^{-1}$] for $(Zn_xMn_{1-x})Fe_2O_4$ and $(Zn_xFe_{1-x})Fe_2O_4$ with different concentrations. Data were taken from the literature.[84]

| $(Zn_xMn_{1-x})Fe_2O_4$ | | | | | | |
|---|---|---|---|---|---|---|
| $x$ | 0.0 | 0.1 | 0.2 | 0.3 | 0.4 | 0.8 |
| $M_s$ | 125 | 140 | 154 | 166 | 175 | 137 |
| $r2$ | 422 | 516 | 637 | 754 | 860 | 388 |
| $(Zn_xFe_{1-x})Fe_2O_4$ | | | | | | |
| $x$ | 0.0 | 0.1 | 0.2 | 0.3 | 0.4 | 0.8 |
| $M_s$ | 114 | 126 | 140 | 152 | 161 | 115 |
| $r2$ | 276 | 397 | 466 | 568 | 687 | 307 |

Hybrid $Fe_3O_4$@Au NPs are appealing since they can provide a multimode platform surface for use as contrast-enhanced agents in imaging techniques, but that also possess a magnetic core that can be used as a magnetic nanoheater.[83]

With the aim of obtaining multimode MNPs, Smolensky et al.[65] reported the synthesis and characterization of hybrid $Fe_3O_4$@OAc@Au NPs with an intermediate organic layer to prevent the migration of gold atoms. With a gold-shell thickness of 7.7 nm, the SPR located at 528 nm allows the use of the NPs for dark-field spectroscopy and surface-enhanced Raman spectroscopy (ERS). In addition, their high saturation magnetization of 81 $A m^2 kg^{-1}$ and transverse and longitudinal relaxivity of $r_2$ = 90.9 $mM_{Fe}^{-1}s^{-1}$ and $r_1$ = 10.3 $mM_{Fe}^{-1}s^{-1}$, respectively, which are higher than those of commercially available agents, offer the possibility of using them simultaneously as MRI contrast agents. These multimode MNPs therefore combine MH with different imaging possibilities within a single core–shell design.

In another study, Sotiriu et al.[85] developed hybrid plasmonic superparamagnetic nanoaggregates (50–100 nm) composed of $Fe_3O_4$@$SiO_2$ mixed with Au (30 nm) NPs. By tuning the $SiO_2$ coating shell and Au interparticle distances, their plasmonic coupling was able to be controlled to place absorption in the near-IR region (transmittance window for human tissues). The MRI ability was assured by a transversal relaxivity $r_2$ = 325 $mM_{Fe}^{-1}s^{-1}$ at 4.7 T superior to commercially available agents with similar sizes, and also MH is affordable within the reported value of saturation magnetization around 50 emu $g^{-1}$.

## 5. Conclusion

Hierarchical core–shell architectures can be obtained by coating magnetic material with several agents (polymers, drugs, proteins, etc.) to allow for multipurpose applications including magnetic hyperthermia, MRI or tissue engineering within a single design.

Following designed criteria that emerge from the interaction at the nano–bio interface, a core with superior magnetic quality and an outer shell with therapeutic-added values and protein corona-evading abilities are all a must for successful use in MH biological applications.

A plethora of different iron oxide based magnetic cores and shells comprising different polymers (PEG, PAA, PNIPAM, etc.) or inorganic shells ($SiO_2$, Au, etc.) loaded with tagging (peptides, aptamers, etc.) and therapeutic agents can be found in the literature; they show interesting therapeutical effects (see Table 3) and evidence the large degree of maturity attained in the field of NP chemical synthesis. Core@shell NPs with well-controlled size, shape and crystalline quality can be synthesised even in one-pot procedures.

Table 3. Summary of NPs with a design strategy that show superior multifunctional abilities for MH-based biological applications.

| Ref. | NP strategy | Application |
|---|---|---|
| [84] | Zn- and Mn-doped $Fe_3O_4$ cores | combined MRI and MH with superior performance. |
| [65] | $Fe_3O_4$@Au | enhanced Raman spectroscopy & MRI & MH. |
| [56] | bipyridium–$Fe_3O_4$ | stable for large pH variations pH = 1, 11. |
| [11] | PEG-decorated $Fe_3O_4$ | high opsonization avoidance with enhanced tagging. |
| [44] | Co-doped $Fe_3O_4$ in Fn cage | specific tagging of melanoma cells and MH. |
| [62] | PNIPAM/chitosan and $Fe_3O_4$ NC | sharp controlled drug delivery and MH. |
| [77–80] | FeHA/PCL magnetic scaffolds | tissue engineering with magnetic scaffolds allowing for MH, MRI and EDD. |

Although the killing of tumour cells is one of the most explored MH-based applications of core@shell MNPs, tissue regeneration or enhanced drug delivery combined with MRI can also be achieved by following design criteria. Examples of brain cancer studies in phase II clinical trials, bone-tissue engineering materials tested in vivo, and controlled release (1 s) of curcumin in PNIPAM/chitosan are only a few of the large list of reported MH applications under development.

## Acknowledgments

This work was financially supported by the European Commission through FEDER and FP7 programs (0681_InveNNta_1_E; Future NanoNeeds-N. 604602), by the Spanish Ministerio de Ciencia e Innovación (MICINN) (MAT2010-20442, MAT2011-28673-C02-01), by the Spanish Ministerio de Economía y Competitividad (MINECO) (MAT2012-36754-C02-01), and by the Xunta de Galicia, Spain (GRC2013-044, FEDER Funds).

[1] Q. A. Pankhurst, J. Connolly, S. K. Jones, J. Dobson, *J. Phys. D* **2003**, *36*, R167–R181.
[2] S. Laurent, D. Forge, M. Port, A. Roch, C. Robic, L. Vander Elst, R. N. Muller, *Chem. Rev.* **2008**, *108*, 2064–2110.
[3] C. G. Hadjipanayis, M. J. Bonder, S. Balakrishnan, X. Wang, H. Mao, G. C. Hadjipanayis, *Small* **2008**, *4*, 1925–1929.
[4] D. Ortega, Q. A. Pankhurst, *Magnetic Hyperthermia*, in: *Nanoscience*, vol. 1: *Nanostructures through Chemistry* (Ed.: P. O'Brien), Royal Society of Chemistry, Cambridge, UK, **2013**, p. 60–68.
[5] O. Petracic, *Superlattices Microstruct.* **2010**, *47*, 569–578.
[6] R. B. Campbell, *Nanomedicine* **2007**, *2*, 649–652.
[7] A. K. Gupta, R. R. Naregalkar, V. Deep Vaidya, M. Gupta, *Nanomedicine* **2007**, *2*, 23–39.
[8] R. Langer, *Science* **1990**, *249*, 1527–1533.
[9] I. Lynch, K. A. Dawson, *Nanotoday* **2008**, *3*, 40–47.
[10] S. Mornet, S. Vasseur, F. Grasset, E. Duguet, *J. Mater. Chem.* **2004**, *14*, 2161–2175.
[11] R. Gref, M. Luck, P. Quellec, M. Marchand, E. Dellacherie, S. Harnisch, T. Blunk, R. H. Muller, *Colloids Surf. B* **2000**, *18*, 301–313.
[12] S. Tenzer, D. Docter, J. Kuharev, A. Musyanovych, V. Fetz, R. Hecht, F. Schlenk, D. Fischer, K. Kiouptsi, C. Reinhardt, K. Landfester, H. Schild, M. Maskos, S. K. Knauer, R. H. Stauber, *Nat. Nanotechnol.* **2013**, *8*, 772–781.
[13] M. Rahman, S. Laurent, N. Tawil, L. Yahia, M. Mahmoudi, *Protein–Nanoparticle Interactions: The Bio–Nano Interface*, Springer Series in Biophysics **2013**, *15*, 21–44.
[14] R. M. Pearson, V. V. Juettner, S. Hong, *Front. Chem.* **2014**, *2*, 108(1:7).
[15] C. Boyer, M. R. Whittaker, V. Bulmus, J. Liu, T. P. Davies, *NPG Asia Mater.* **2010**, *2*, 23–30.
[16] X. Trepat, L. Deng, S. S. An, D. Navajas, D. J. Tschumperlin, W. T. Gerthoffer, J. P. Butler, J. J. Fredberg, *Nature* **2007**, *447*, 592–596.
[17] X. Trepat, M. R. Wasserman, T. E. Angelini, E. Millet, D. A. Weitz, J. P. Butler, J. J. Fredeberg, *Nature Phys.* **2009**, *5*, 426–430.
[18] S. Baek, X. Quan, S. Kim, C. Lengner, J.-K. Park, J. Klim, *ACSNano* **2014**, *8*, 10125–10138.
[19] M. Pesce, A. Patruno, L. Speranza, M. Reale, *Eur. Cytokine Network* **2013**, *24*, 1–10.
[20] A. Tefferi, *Curr. Hematol. Rep.* **2003**, *2*, 237–241.
[21] M. K. Kuimova, *Phys. Chem. Chem. Phys.* **2012**, *14*, 12671–12682.
[22] K. Comley, N. A. Fleck, *Int. J. Solids Struct.* **2010**, *47*, 2982–2990.
[23] B. Hildebrandt, P. Wust, O. Ahlers, A. Dieing, G. Sreenivasa, T. Kerner, R. Felix, H. Riess, *Crit. Rev. Oncol. Hematol.* **2002**, *43*, 33–56.
[24] M. T. Huff, Y. N. Tong, L. M. Zhao, J. W. Hansen, K. X. Cheng, A. A. Wei, *Nanomedicine* **2007**, *2*, 125–132.
[25] C. Minelli, S. B. Lowe, M. S. Stevens, *Small* **2010**, *6*, 2336–2357.
[26] R. E. Rosensweig, *J. Magn. Magn. Mater.* **2002**, *25*, 2:370–374.
[27] R. Hergt, S. Dutz, M. Ziesberger, *Nanotechnology* **2010**, *21*, 015706.
[28] J. Carrey, B. Mehdaoui, M. Respaud, *J. Appl. Phys.* **2011**, *109*, 083921(1–17).
[29] J. Rivas, M. Bañobre-López, Y. Piñeiro-Redondo, B. Rivas, M. A. López-Quintela, *J. Magn. Magn. Mater.* **2012**, *324*, 3499–3502.
[30] M. A. Gonzalez-Fernandez, T. Torres, M. Andres-Verges, R. Costo, P. de la C. J. Presa, M. P. Serna, C. Morales, M. R. Marquina, G. F. Ibarra, *J. Solid State Chem.* **2009**, *182*, 2779–*2784*.
[31] Y. Piñeiro-Redondo, M. Bañobre-López, I. Pardiñas-Blanco, G. Goya, M. A. López-Quintela, J. Rivas, *Nanoscale Res. Lett.* **2011**, *6*, 383.

 

[32] P. H. Linh, P. V. Thach, N. A. Tuan, N. C. Thuan, D. H. Mahn, N. X. Phuc, *J. Phys. Conf., Ser.* **2009**, *187*, 012069(1–5).
[33] A. Uritzberea, E. Natividad, A. Arizaga, M. Castro, A. Mediano, *J. Phys. Chem. C* **2010**, *114*, 4916–4922.
[34] C. Martinez-Boubeta, K. Simeonidis, D. Serantes, I. Conde-Leborán, I. Kazakis, G. Stefanou, L. Peña, R. Galceran, L. Balcells, C. Monty, D. Baldomir, M. Mitrakas, M. Angelakeris, *Adv. Funct. Mater.* **2012**, *22*, 1.
[35] M. Bañobre-López, Y. Piñeiro Redondo, M. A. López-Quintela, J. Rivas, "Magnetic Nanoparticles for Biomedical Applications", in: *Handbook of Nanomaterials Properties* (Eds.: B. Bhushan, D. Luo, S. Schricker, W. Sigmund, S. Zauscher), Springer-Verlag, Heidelberg, Germany, **2014**, chapter 15.
[36] V. K. LaMer, R. Dinegar, H. Theory, *J. Am. Chem. Soc.* **1950**, *72*, 4847–4854.
[37] Y. Kolen'ko, M. Bañobre-López, C. Rodriguez-Abreu, E. Carbo-Argibay, A. Sailsman, Y. Piñeiro-Redondo, M. F. Cerqueira, D. Petrovykh, K. Kovnir, O. Lebedev, J. Rivas, *J. Phys. Chem. C* **2014**, *118*, 8691–8701.
[38] T. S. S. Hyeon, J. Lee, Y. Park, H. B. Chung, *J. Am. Chem. Soc.* **2001**, *123*, 12798–12801.
[39] M. A. López-Quintela, *Curr. Opin. Colloid Interface Sci.* **2003**, *8*, 137–144.
[40] J. Vidal-Vidal, J. Rivas, M. A. López-Quintela, *Colloids Surf. A* **2006**, *288*, 44–51.
[41] T. J. Daou, G. Pourroy, S. Begin-Colin, C. Greneche, J. M. Ulhaq-Bouillet, P. Legare, P. Bernhardt, C. Leuvrey, G., Rogez, *Chem. Mater.* **2006**, *18*, 4399–4404.
[42] M. Uchida, L. O. Liepold, T. Douglas, *Protein Cage Magnetic Nanoparticles*, in: *Magnetic Nanoparticles from Fabrication to Clinical Applications* (Ed.: N. T. K. Thanh), CRC Press, Taylor and Francis, Boca Raton, FL, USA, **2012**, p. 73–95.
[43] F. C. Meldrun, V. J. Wade, D. L. Nimmo, B. R. Heywood, S. Mann, *Nature* **1991**, *349*, 684–687.
[44] E. Fantechi, C. Innocenti, M. Zanardelli, M. Fittipaldi, E. Falvo, M. Carbo, V. Shullani, L. Cesare Manelli, C. Ghelardini, A. M. Ferret, A. Ponti, C. Sangregorio, P. Ceci, *ACSNano* **2014**, *8*, 4705–4719.
[45] M. J. Parker, M. A. Allen, B. Ramsay, M. T. Klem, M. Young, T. Douglas, *Chem. Mater.* **2008**, *20*, 1541–1547.
[46] J. Verma, S. Lal, C. J. F. van Noorden, *Int. J. Nanomed.* **2014**, *9*, 2863–2877.
[47] H. Lee, T. J. Yoon, R. Weissleder, *Angew. Chem. Int. Ed.* **2009**, *48*, 5657–5660; *Angew. Chem.* **2009**, *121*, 5767.
[48] W. Wu, Q. He, C. Jiang, *Nanoscale Res. Lett.* **2008**, *3*, 397–415.
[49] H. Quanguo, Z. Lei, W. Wei, H. Rong, H. Jingke, *Sensors* **2010**, *22*, 285–295.
[50] M. H. Mashhadizadeh, M. Amoli-Diva, *Nanomedicine* **2012**, *3*, 1000139(1:7).
[51] Y. Sahoo, H. Pizem, T. Fried, D. Golodnitsky, L. Burstein, C. N. Sukenik, G. Markovich, *Langmuir* **2001**, *17*, 7907–7911.
[52] A. K. Gupta, M. Gupta, *Biomaterials* **2005**, *26*, 3995–4021.
[53] P. Guardia, B. Batlle-Brugal, A. G. Roca, O. Iglesias, M. P. Morales, C. J. Serna, A. Labarta, X. Batlle, *J. Magn. Magn. Mater.* **2007**, *316*, e756.
[54] N. A. Frey, S. Peng, K. Cheng, S. Sun, *Chem. Soc. Rev.* **2009**, *38*, 2532–2542.
[55] S. H. Sun, H. Zeng, D. B. Robinson, S. Raoux, P. M. Rice, S. X. Wang, G. X. Li, *J. Am. Chem. Soc.* **2004**, *126*, 273–279.
[56] J. Fan, J. Lu, R. Xu, R. Jiang, Y. Gao, *J. Colloid Interface Sci.* **2003**, *266*, 215–218.
[57] M. Lattuada, T. A. Hatton, *Langmuir* **2007**, *23*, 2158–2168.
[58] T.-M. Liu, J. Yu, C. A. Chang, A. Chiou, H. K. Chiang, Y.-C. Chuang, C.-H. Wu, C.-H. Hsu, P.-A. Chen, C.-C. Huang, *Sci. Rep.* **2014**, *4*, 5593(1:10).
[59] X. Lu, M. Niu, R. Qiao, M. Gao, *J. Phys. Chem. B* **2008**, *112*, 14390–14394.
[60] J. F. Lutz, S. Siller, A. Hoth, L. Kaufner, U. Pison, R. Cartier, *Biomacromolecules* **2012**, *7*, 3132–3138.
[61] J.-O. You, D. Almeda, G. J. C. Ye, D. T. Auguste, *J. Biol. Eng.* **2010**, *4*, (1:15).
[62] T. Yadavalli, S. Ramasamy, G. Chandrasekaran, I. Michael, H. A. Therese, R. Chennakesavulu, *J. Magn. Magn. Mater.* **2015**, *380*, 315–320.
[63] C. Dionigi, Y. Piñeiro, A. Riminucci, M. Bañobre, J. Rivas, V. Dediu, *Appl. Phys. A* **2014**, *114*, 585–590.
[64] J. Rivas, Y. Piñeiro, E. Iglesias-Silva, J. M. Vilas-Vilela, L. M. León, A. López-Quintela, *J. Korean Phys. Soc.* **2013**, *62*, 1376–1381.
[65] E. D. Smolenski, M. C. Neary, Y. Zhou, T. S. Berquo, V. C. Pierre, *Chem. Commun.* **2011**, *47*, 2149–2151.
[66] L. León-Félix, J. Chaker, M. Parise, J. A. H. Coaquira, L. De Los Santos Valladares, A. Bustamante, V. K. Garg, A. C. Oliveira, P. C. Morais, *Hyperfine Interact.* **2014**, *224*, 179–188.
[67] R. G. Digigow, J.-F. Dechéllez, H. Dietsch, I. Geissbühler, D. Vanhecke, C. Geers, A. M. Hirt, B. Rothen-Rutishauer, *J. Magn. Magn. Mater.* **2014**, *362*, 72–79.
[68] S. Dutz, R. Hergt, *Nanotechnology* **2014**, *25*, 452001(1:28).
[69] www.magforce.com.
[70] D. Ortega, Q. Pankhurst, *Magnetic Hyperthermia*, in: *Nanoscience*, vol. 1: *Nanostructures through Chemistry* (Ed.: P. O'Brien), Royal Society of Chemistry, Cambridge, **2013**, p. 60–68.
[71] H. Skaat, S. Margel, *J. Biotechnol. Biomater.* **2013**, *3*, 1000156(1:8).
[72] M. Glat, H. Skaat, N. Menkes-Casp, S. Margel, E. A. Stern, *J. Nanobiotechnol.* **2013**, *11*, 32(1–12).
[73] R. Regmi, S. R. Bhattarai, C. Sudakar, C. S. Wani, R. Cunningham, P. P. Vaishnava, R. Naik, D. Oupicky, G. Lawes, *J. Mater. Chem.* **2010**, *20*, 6158–6163.
[74] A. Matsumine, K. Takegami, K. Asanuma, T. Matsubara, T. Nakamura, A. Uchida, A. Sudo, *Int. J. Clin. Oncol.* **2011**, *16*, 101–108.
[75] R. Sensenig, Y. Sapir, C. MacDonald, S. Cohen, B. Polyak, *Nanomedicine* **2012**, *7*, 1425–1442.
[76] J. Chen, Z.-D. Shi, X. Ji, J. Morales, J. Zhang, N. Kaur, S. Wang, *Tissue Eng.* **2013**, *19*(5–6), 716–728.
[77] A. Gloria, T. Russo, U. D'Amora, S. Zeppetelli, R. De Santis, T. D'Alessandro, M. Sandri, M. Bañobre-López, Y. Piñeiro-Redondo, M. Uhlarz, L. Ambrosio, A. Tampieri, J. Rivas, T. Herrmannsdörfer, *J. Roy. Soc. Interface* **2013**, *10*, 20120833.
[78] A. Tampieri, T. D'Alessandro, M. Sandri, S. Sprio, E. Landi, L. Bertinetti, S. Panseri, G. Pepponi, J. Goettlicher, M. Bañobre-López, J. Rivas, *Acta BioMater.* **2012**, *8*, 843–851.
[79] M. Bañobre-López, Y. Piñeiro-Redondo, R. De Santis, A. Gloria, L. Ambrosio, A. Tampieri, V. Dediu, J. Rivas, *J. Appl. Phys.* **2011**, *109*, 07B313.
[80] M. Bañobre-López, Y. Piñeiro-Redondo, M. Sandri, A. Tampieri, R. De Santis, V. A. Dediu, J. Rivas, *IEEE Trans. Magn.* **2014**, *50*, 5400507(1–7).
[81] S. Panseri, C. Cunha, T. D'Alessandro, M. Sandri, A. Russo, G. Giavaresi, M. Marcacci, C. T. Hung, A. Tampieri, *PLoS ONE* **2012**, *7*, e38710.
[82] S. Panseri, A. Russo, M. Sartori, G. Giavaresi, M. Sandri, M. Fini, M. C. Maltarello, T. Shelyakova, A. Ortolani, A. Visani, V. Dediu, A. Tampieri, M. Marcacci, *Bone* **2013**, *56*, 432–439.
[83] M. Carril, I. Fernández, J. Rodriguez, I. García, S. Peñadés, *Part. Part. Syst. Charact.* **2014**, *31*, 81–87.
[84] J.-T. Jang, H. Nah, J. H. lee, S. h. Moon, M. G. Kim, J. Cheon, *Angew. Chem. Int. Ed.* **2009**, *48*, 1234–1238; *Angew. Chem.* **2009**, *121*, 1260.
[85] G. A. Sotiriou, F. Starsich, A. Dasargayri, M. C. Wuring, F. Krumeich, A. Boss, J.-C. Leorux, S. E. Pratsinis, *Adv. Funct. Mater.* **2014**, *24*, 2818–2827.

Received: June 2, 2015
Published Online: August 20, 2015

 